

# Quantum enhanced agents

M. J. Kewming,<sup>\*</sup> S. Shrapnel, and G. J. Milburn<sup>†</sup>

*Centre for Engineered Quantum Systems, School of Mathematics and Physics, University of Queensland, QLD 4072 Australia*

(Dated: July 10, 2020)

The concept of an embodied intelligent agent is a key concept in modern AI and robotics [1]. Physically, an agent—like a Turing machine—is an open system embedded in an environment which it interacts with through sensors and actuators [2]. It contains a learning algorithm that correlates the sensor and actuator results by learning features about its environment. The sensor-actuator system is similar to a measurement based control system. Quantum mechanics enables new measurement and control protocols capable of exceeding what can be achieved classically [3, 4]. We demonstrate how quantum optical sensors and actuators can dramatically improve an agent’s ability to learn in a thermal environment. Furthermore we use the Jarzynski equality [5] to show that learning maximises the exchange in free energy  $\Delta F$  between the agent’s sensor and actuator when considered as a stochastic feedback cycle.

Machine learning (ML), AI and quantum physics are current hotbeds of academic research. It is unquestionable that the physical sciences have benefited tremendously by incorporating the tools of ML [6]. Recent research has proposed enhancing ML tools and techniques using quantum physics [7–9]. However, more topical research suggests that ML on an industrial scale can have very tangible thermodynamic costs [10]. This suggests it is imperative we develop a deeper understanding of the thermodynamic cost of learning. Recent results using stochastic thermodynamics have obtained fundamental bounds on the efficiency of learning algorithms [11, 12]. Others have also shown that learning maximises the work done by a Maxwell’s demon [13]. This suggests that learning, like other physical process may take place out of thermal equilibrium [14]. For an agent to learn it must interact with the world via physical sensors and actuators which too are thermodynamic processes. Given the known advantages of quantum metrology [3, 4], we consider the improvements that a simple AI endowed with quantum mechanical hardware—otherwise referred to as a quantum enhanced agent—may yield.

Learning requires building models of an external environment using sensory data. Thus, like many other physical processes, learning takes place out of thermal equilibrium. An agent has access to a large reservoir of free energy which it uses to probe its environment. It converts this energy into work which can then be used for learning. We study the thermodynamics of a quantum agent through the lens of quantum machines and molecular systems [15, 16]. A seminal result in non-equilibrium thermodynamics is the Jarzynski equality [17]

$$\langle e^{-W\beta} \rangle = e^{-\Delta F\beta}, \quad (1)$$

which relates the free energy difference  $\Delta F$  between two thermodynamic states to the irreversible work  $W$  required to drive it between the two at inverse temperature  $\beta = 1/k_B T$ . Here we use this equality to calculate the free energy required for a quantum agent to probe its environment.

In our conception, the agents sensor has two states: accept or error. These two outcomes signify agreement or disagreement of its prediction—which can be change—and the observation of the world. The prediction is updated by minimising the probability of measuring an error which is physically similar to the well known optimisation algorithm gradient descent (GD). The measured overlap between the agents prediction and observations define a cost function  $C$ , with the learning rate  $l$  that are fixed by the physical parameters of the system. A schematic of our model is depicted in figure (1a).

In our example a quantum agent uses the temporal profile of a single photon to probe a very restricted environment composed of a single unknown optical element such as an optical cavity. Single photons are highly non-classical states of light, unlike coherent light pulses [18] which contain on average one photon but with Poissonian intensity fluctuations [19, 20]. We use these two sources of light to investigate the difference between classical and quantum agents. There are a number of demonstrated schemes for single photon sources and detectors [21–23]. Here we employ a three-wave-mixing Raman transition for each [24, 25].

In the Raman model, a three level atom is placed inside a single-sided cavity. Two-long lived states  $|g\rangle$  and  $|e\rangle$  are coupled by a third radiative state  $|b\rangle$ . A strong classical electromagnetic control pulse  $E(t)$  is applied to the ground state  $|g\rangle$  at frequency  $\Omega$ . The pulse is detuned from the atomic transition  $|g\rangle \rightarrow |b\rangle$  ensuring the the radiative state is never significantly populated. The resonance condition is  $\Omega - \omega_a = \omega_\sigma$ , where  $\hbar\omega_\sigma$  is the energy difference between  $|g\rangle$  and  $|e\rangle$ . The transition  $|g\rangle \rightarrow |e\rangle$  is mediated by the emission of a photon at frequency  $\omega_a$  as depicted in figure (1b).

In the interaction picture under the rotating wave approximation, the Hamiltonian describing this model is  $H = \hbar E(t)a^\dagger\sigma_+ + \hbar E^*(t)\sigma_-a$  where  $a^\dagger(a)$  are the internal cavity mode creation (annihilation) operators and  $\sigma_+(\sigma_-)$  are the raising (lowering) operators in the subspace formed  $|g\rangle$  and  $|e\rangle$ . At a finite temperature, the

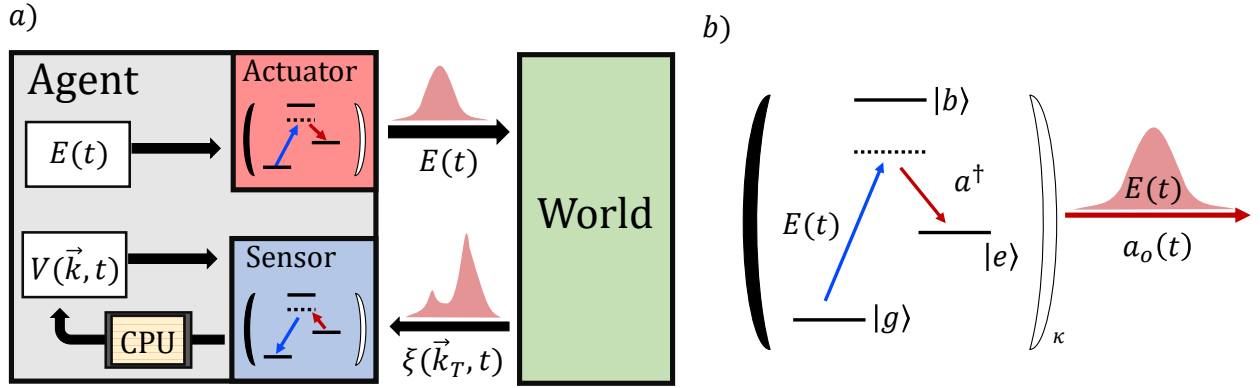


FIG. 1. (a) Depiction of a learning agent interacting with the world b). The agent houses both an actuator and sensor which it uses to probe and measure the world. The actuator is maintained at a positive temperature equilibrium state (red) while the sensor is maintained in a negative temperature equilibrium state (blue). The agent emits photons with a temporal profile  $E(t)$  which is perturbed by the environment transforming it to  $\xi(\vec{k}_T, t)$ . The sensor will maximally absorb the photon when its control field  $V(\vec{k}, t)$  matches the incoming pulse. (b) The Raman model inside the actuator and sensor. It includes a three level atom enclosed in a singled-sided cavity with decay rate  $\kappa$ . A strong, but highly detuned classical driving field couples the two long lived ground states  $|g\rangle$  and  $|e\rangle$  via the virtual transition with the radiative state  $|b\rangle$ . Single photons are then emitted to into the output mode  $a_o(t)$  with a temporal profile determined by the control. In the detector model this process is reversed and an incoming photon is perfectly absorbed when a single photon has the same temporal shape as the control field.

evolution of the cavity-atomic joint state is governed by the master equation (ME)

$$\frac{d\rho}{dt} = -i[H, \rho] + \kappa(\bar{n} + 1)\mathcal{D}[a]\rho + \kappa\bar{n}\mathcal{D}[a^\dagger]\rho \quad (2)$$

where  $\kappa$  is the decay rate of the cavity mode into the environment,  $\bar{n}$  is the mean photon number in the environment and  $\mathcal{D}[a]\rho = a\rho a^\dagger - \{a^\dagger a, \rho\}/2$  is the Lindblad dissipator. We have neglected decay between  $|e\rangle \rightarrow |g\rangle$  with the assumption that the atomic decay rate is much slower than the intra-cavity mode  $\kappa$ . We further assume the atom-cavity system is initially in thermal equilibrium with the environment thus, in a separable thermal Gibbs states  $\rho_{\text{sys}} = \bar{\rho}_a \otimes \bar{\rho}_\sigma$  with Boltzman factors  $\mu_i = \hbar\omega_i/k_B T$ . Thermal equilibrium ensures  $\mu_a = \mu_\sigma$ .

A reliable quantum actuator requires two things; sufficient control over the shape of the output field  $a_o(t)$  and the photon number  $a_o^\dagger(t)a_o(t)$ . We use the quantum Langevin equations to describe the stochastic evolution of the intracavity  $a(t)$  in terms of the input  $a_i(t)$  and output fields  $a_o(t)$  [18, 26]. The output field is—on average—the convolution of the cavity response and the product of the control field amplitude and atomic polarisation  $\langle a_o(t) \rangle = -i\sqrt{\kappa} \int_0^t dt' \exp(\kappa(t' - t)/2) E(t') \langle \sigma_+(t') \rangle$ . Therefore, controlling the classical drive  $E(t)$  shapes the overall response of the source.

A reliable single photon source will operate in the limit of a large cavity decay rate  $\kappa$  and thus preferentially emit into the environment. In this limit, we can adiabatically eliminate the cavity dynamics, which after a long time  $t \gg 0$  yields a vanishing output mode  $\langle a_o(t) \rangle = 0$  but with the mean photon number  $\langle a_o^\dagger(t)a_o(t) \rangle = \bar{n} +$

$4|E(t)|^2 \langle \sigma_z(t) \rangle / \kappa$  where  $\langle \sigma_z(t) \rangle = \tanh(\mu_\sigma/2)$  and  $\bar{n}$  is the mean photon number of the thermal environment. At zero temperature this is consistent with a single photon Fock-state in the output field where the temporal profile is determined by the control field  $E(t)$ .

In the classical model, the agent pumps directly into the environment with a coherent pulse. The mean output-mode in this model is  $\langle a_o(t) \rangle = -i \int_0^t dt' E(t')$  with a mean photon number  $\langle a_o^\dagger(t)a_o(t) \rangle = \bar{n} + \int_0^t dt' |E(t')|^2$ .

We will further assume the actuator pulse returns to the detector after its temporal profile is perturbed unitarily  $E(t) \rightarrow \xi(\vec{k}_T, t)$ ; here the true discoverable parameters  $\vec{k}_T$  determine the measurable effect of the environment on the pulse. The actuator model can be suitably adapted into a detection model by reversing the process. The virtual transition between the  $|g\rangle$  and  $|e\rangle$  is again mediated by a classical control field—denoted  $V(\vec{k}, t)$  where  $\vec{k}$  are the control parameters determining its temporal profile. The sensor requires a source of energy to ensure a population inversion; the excited state  $|e\rangle$  is now preferentially populated, creating a negative temperature equilibrium states satisfying  $\mu_a = -\mu_\sigma$  [27]. A successful detection occurs when an incoming photon at frequency  $\omega_a$  is absorbed and de-excites the atom into the ground state  $|g\rangle$ .

We cannot describe the absorption process via the standard ME equation (2), but rather the Fock-state master equations [28]. In this framework, the entire system is described by a joint system  $\rho = \rho_{\text{sys}} \otimes |1_\xi\rangle\langle 1_\xi|$  where the incoming photon is in a single photon Fock-state. This interaction with the single-sided cavity is

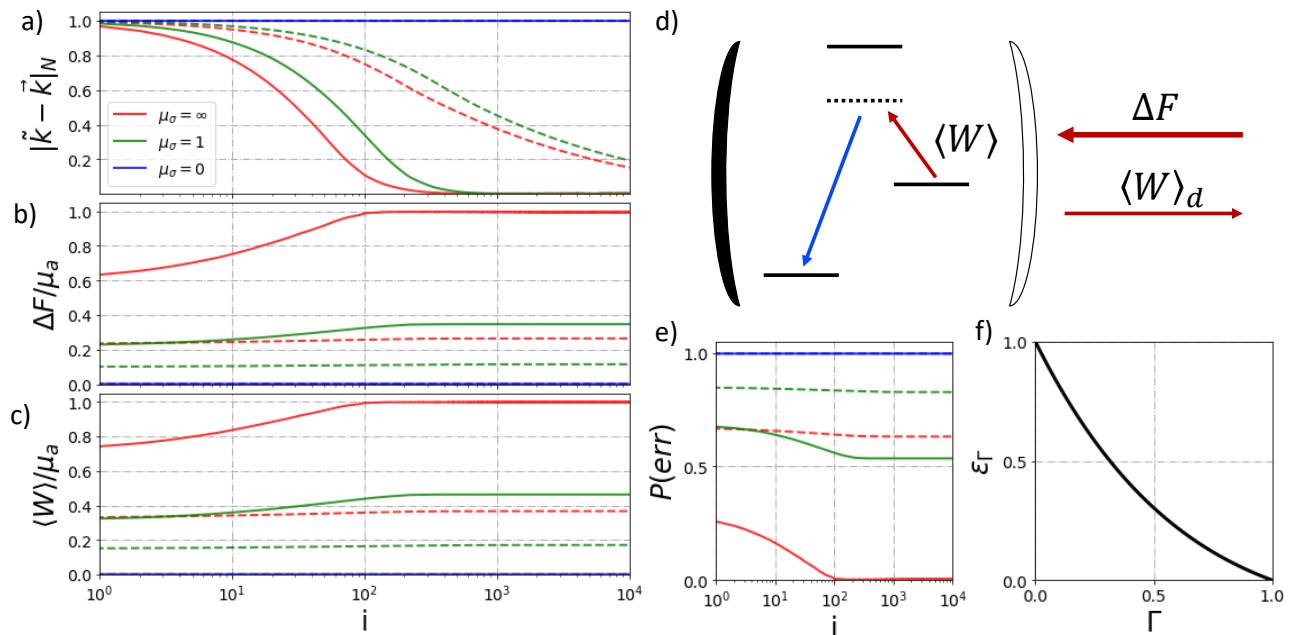


FIG. 2. (a) The normalised parameter difference—each parameter is dimensionless between 0 and 1—of the agents prediction and observation defined  $|\vec{k} - \vec{k}_T|_N$  as a function of iterations  $i$ . The quantum agent (solid) outperforms the classical agent (dashed) at all temperatures excluding the infinite temperature limit  $\mu_\sigma \rightarrow 0$ . (b) and (c) show the scaled free energy  $\Delta F/\mu_a$  and average work done  $\langle W \rangle$  transferred between emitted pulse after interacting with the environment and the agent. As the agent's estimate  $\vec{k}$  improves, the change in free energy and work done are maximised. As the temperature increases the amount of energy exchanged decreases in both models. (d) As the temperature increases, the detector is more likely to be in the error state leading to an increase in dissipated work  $\langle W \rangle_d$  which cannot be used for learning. (e) The probability of measuring an error in the incoming pulse  $\xi(\vec{k}_T, t)$ . When the estimate is incorrect  $\Gamma < 1$  the probability of the atom de-exciting into the ground state is not guaranteed. As the agents estimate improves, the probability of obtaining an error decreases. (f) The exponential dependence on  $\Gamma$  in the classical model introduces a variable learning rate  $\epsilon_\Gamma$  as a function of the overlap  $\Gamma$ . As the agents estimate of the parameters  $\vec{k}$  approach the true values—and  $\Gamma \rightarrow 1$ —the classical agent can no longer resolve minor changes in due to the intrinsic photon number uncertainty in the probe.

described via the coupled set of ME's

$$\frac{d\rho_{m,n}}{dt} = \mathcal{L}\rho_{m,n} + \sqrt{m}\sqrt{\kappa\eta}\xi(k,t) [\rho_{m-1,n}, a^\dagger] + \sqrt{n}\sqrt{\kappa\eta}\xi^*(k,t) [a, \rho_{m,n-1}], \quad (3)$$

where  $\eta$  is the quantum efficiency of the detector and also accounts for loss in the environment and  $m$  and  $n$  are integers. The equation for  $\rho_{0,0}$  is identical to the vacuum master equation (2) and can be solved in principle. The diagonal elements  $\rho_{n,n}$  are initialised with  $\rho_{\text{sys}}(0)$  whereas the off-diagonal elements are initialised to zero.

In the single-photon Raman model a successful detection occurs when the atom is measured in the ground state  $|g\rangle$ . For example, this could be done accurately with negligible dissipation using fluorescent imaging [24]. The probability of finding the atom in the ground state in the long time limit  $t \gg 0$  is

$$P_g^{(Q)}(t) = \frac{1}{1 + e^{\mu_\sigma}} + \frac{4\eta\Gamma}{\kappa} \tanh\left(\frac{\mu_\sigma}{2}\right), \quad (4)$$

where  $\Gamma = \left| \int dt' V^*(\vec{k}, t') \xi(\vec{k}_T, t') \right|^2$  measures the over-

lap of the two fields and is maximised when  $V^*(\vec{k}, t) = \xi(\vec{k}_T, t)$  and the  $Q$  superscript signifies this is the quantum model. The first term corresponds to the conditional probability of absorbing a thermal photon  $P_{g|T}^{(Q)}(t)$ , whereas the second term is the conditional probability of absorbing the signal photon  $P_{g|\xi}^{(Q)}(t)$ .

In the classical model we replace the single photon pulse by an incoming coherent state with temporal shape  $\xi(\vec{k}_T, t)$ . The Fock-state master equation (3) is modified to the initial master equation (2) with an additional coherent drive term. Furthermore, the conditional probability of measuring the atom in the ground state from such pulse is

$$P_g^{(C)}(t) = \frac{1}{1 + e^{\mu_\sigma}} + \frac{4\eta\Gamma}{\kappa} e^{-4\eta\Gamma/\kappa} \tanh\left(\frac{\mu_\sigma}{2}\right) \quad (5)$$

where the superscript  $C$  signifies this is the classical model. Thus, the primary difference between the classical model and the quantum model is due to the exponential dependence on overlap  $\Gamma$  which is due to the intensity fluctuations in the coherent field [18]. The derivation of

all these results can be found in the supplementary material.

We assume the agent and the environment are materially identical—otherwise known as the principle of requisite variety—so matching  $V(\vec{k}, t)$  and  $\xi(\vec{k}_T, t)$  requires matching the parameters  $\vec{k}$  and  $\vec{k}_T$ .

For each experimental run  $i$ , the agent measures the detector in the ground or excited state, both of which register a classical bit of information  $x_i \in \{0, 1\}$  respectively. When the agent's control pulse  $V(\vec{k}, t)$  perfectly overlaps the worlds  $\xi(\vec{k}_T, t)$ , the probability of measuring and error (excited state)  $P_e(t) = 1 - P_g(t)$  is minimised. For  $N$  trials,  $x_i$  is a binary random variable with mean  $\bar{x}_N = \sum_{i=0}^N x_i/N$  which in the limit of large  $N$  approaches  $\bar{x}_N \rightarrow P_e(t)$  with variance  $\Delta x = \bar{x}_N(1 - \bar{x}_N)$ .

The agent updates its estimate  $\vec{k}$  via constant feedback from  $\bar{x}_N$ . As  $V(\vec{k}, t)$  enters  $P_e(t)$  through  $\Gamma$ , the feedback/learning protocol must maximise  $\Gamma$ . Moreover, we define the error current using the chain rule

$$I(t) = \frac{d\bar{x}_N}{dt} = \frac{d\vec{k}}{dt} \cdot \vec{\nabla}_{\vec{k}} P_e \quad (6)$$

where the learning dynamics are defined numerically between trials as  $d\vec{k}/dt = l(\vec{k}_{i+1} - \vec{k}_i)$  and  $l$  defines the learning rate. The learning rate will be constrained by the physical parameters of the detector i.e by its thermal state  $\mu_\sigma$  and quantum efficiency  $\eta$  as specified in the probability distributions equation (4) and equation (5). Also, each trial is repeated every  $\tau$  seconds, thus the time between each control integration is  $N\tau$ . This further bounds the learning rate below  $1/N\tau$ .

If the agent updates its estimate algorithmically using feedback and gradient descent  $\vec{k}_{i+1} = \vec{k}_i + \kappa \vec{\nabla}_{\vec{k}} P_e$ , we find that the error current  $I(t)$  is minimised when  $\vec{\nabla}_{\vec{k}} P_e \rightarrow 0$  and  $\vec{k}_i = \vec{k}_T$ . Thus, the agent learns the environment by simply minimising the number of observed errors in its measurements protocol.

As an example, suppose the control  $V(\vec{k}, t)$  and input pulses  $\xi(\vec{k}_T, t)$  are exponentially decaying temporal modes i.e  $\xi(\vec{k}_T, t) = \sqrt{\gamma} \exp(-\gamma t/2 + i\Delta t)$  for  $t \geq 0$  generated by an optical cavity with linewidth  $\gamma$  and detuning  $\Delta$ . The convergence between to truth  $\vec{k}_T$  and prediction  $\vec{k}$  can be monitored via the normalised Euclidean distance  $|\vec{k} - \vec{k}_T|_N$  shown in figure (2a). Assuming both models have a fixed learning rate  $l$ , the quantum agent outperforms the classical agent at all temperatures converging on the true estimates an order of magnitude faster  $i$ .

The average work done  $\langle W \rangle / \mu_a$  due to the absorption of a signal photon  $\hbar\omega_a$  is readily computed as shown figure (2c). We can further compute free energy  $\langle \Delta F \rangle / \mu_a$  via the Jarzynski equality equation (1) also shown in figure (2b). As the agent's prediction of the world improves, so to does the conversion change in free energy  $\Delta F$ . At zero temperature  $\mu_a = \infty$  and  $\eta = 1$  we have  $\Delta F \rightarrow \langle W \rangle$  as the agents estimate of the world approaches the true

value  $\vec{k} \rightarrow \vec{k}_T$ . Thus, the free energy emitted from source is perfectly converted to useful work for the task of learning  $\vec{k}_T$ . As the temperature increases,  $\Delta F / \mu_a$  decreases indicating less work is reliably used for learning and more is dissipated back into the environment  $\langle W \rangle_d = \langle W \rangle - \Delta F$  satisfying  $\Delta F \leq \langle W \rangle$  shown in figure (2d) [16].

Lastly, the classical agents capacity to convert free energy  $\Delta F / \mu_a$  into learning is hindered by the fact that weak coherent states are primarily dominated by vacuum i.e no photon was emitted from the actuator. When the error rate— $P_e(t)$ —between the classical and quantum models is roughly equivalent, the convergence rate in the quantum agent is roughly an order of magnitude higher than the classical agent shown in figure (2e). This is due to the variable learning rate which approaches 0 as  $\Gamma \rightarrow 1$  since  $\nabla_{\vec{k}} P_g^P(C) \propto (1 - 4\eta\Gamma/\kappa)e^{-4\eta\Gamma/\kappa} = \epsilon_\Gamma$ . As the classical agent converges on the true values, the intrinsic uncertainty in the probes photon number makes it more difficult to resolve the smaller differences between prediction and observation. This limitation is not present in the quantum model which is limited only in the estimate of the error rate i.e  $1/\sqrt{N}$  [3, 4].

In this contrived model, learning is a thermodynamic process where the work done by an actuator on the environment is maximally converted to useful work on the sensor. Thus, it is conceivable that an agents capacity to learn its environment improves the overall thermodynamic efficiency of transmitting energy from actuators to its sensors. Moreover, we have shown that if these devices are operated at the quantum limit, they achieve a substantial increase in their learning capacity and efficiency over their classical counterparts. This advantage is due entirely to the difference in photon number certainty between each of the two probes.

## ACKNOWLEDGEMENTS

This work was supported by FQXi FFF Grant number FQXi-RFP-1814 and the Australian Research Council Centre of Excellence for Engineered Quantum Systems (Project number CE170100009).

\* m.kewming@uq.edu.au

† millburn@physics.uq.edu.au

- [1] S. J. Russell and P. Norvig, *Artificial Intelligence: A Modern Approach*, 2nd ed. (Pearson Education, 2003).
- [2] R. Penrose, *The Emperors New Mind: Concerning Computers, Minds, and the Laws of Physics* (Oxford University Press, Incorporated, Oxford, UK, 2002).
- [3] V. Giovannetti, S. Lloyd, and L. Maccone, *Nature Photonics* **5**, 222 (2011), number: 4 Publisher: Nature Publishing Group.

- [4] C. Degen, F. Reinhard, and P. Cappellaro, *Reviews of Modern Physics* **89**, 035002 (2017), publisher: American Physical Society.
- [5] C. Jarzynski, *Physical Review E* **56**, 5018 (1997), publisher: American Physical Society.
- [6] G. Carleo, I. Cirac, K. Cranmer, L. Daudet, M. Schuld, N. Tishby, L. Vogt-Maranto, and L. Zdeborov, *Reviews of Modern Physics* **91**, 045002 (2019), publisher: American Physical Society.
- [7] M. Schuld, I. Sinayskiy, and F. Petruccione, *Contemporary Physics* **56**, 172 (2015).
- [8] J. Biamonte, P. Wittek, N. Pancotti, P. Rebentrost, N. Wiebe, and S. Lloyd, *Nature* **549**, 195 (2017), number: 7671 Publisher: Nature Publishing Group.
- [9] M. Schuld and N. Killoran, *Physical Review Letters* **122**, 040504 (2019), publisher: American Physical Society.
- [10] E. Strubell, A. Ganesh, and A. McCallum, arXiv:1906.02243 [cs] (2019).
- [11] S. Goldt and U. Seifert, *Physical Review Letters* **118**, 010601 (2017), publisher: American Physical Society.
- [12] S. Goldt and U. Seifert, *New Journal of Physics* **19**, 113001 (2017).
- [13] A. B. Boyd, J. P. Crutchfield, and M. Gu, arXiv:2006.15416 (2020).
- [14] J. L. England, *Nature Nanotechnology* **10**, 919 (2015), number: 11 Publisher: Nature Publishing Group.
- [15] H. T. Quan, Y.-x. Liu, C. P. Sun, and F. Nori, *Physical Review E* **76**, 031105 (2007), publisher: American Physical Society.
- [16] U. Seifert, *Reports on Progress in Physics* **75**, 126001 (2012), publisher: IOP Publishing.
- [17] C. Jarzynski, *Physical Review Letters* **78**, 2690 (1997), publisher: American Physical Society.
- [18] D. F. Walls and G. J. Milburn, *Quantum Optics*, 2nd ed. (Springer-Verlag, Berlin Heidelberg, 2008).
- [19] I. A. Walmsley, *Science* **348**, 525 (2015).
- [20] G. J. Milburn and S. Basiri-Esfahani, *Proceedings of the Royal Society A: Mathematical, Physical and Engineering Sciences* **471**, 20150208 (2015).
- [21] P. B. R. Nisbet-Jones, J. Dilley, D. Ljunggren, and A. Kuhn, *New Journal of Physics* **13**, 103036 (2011), publisher: IOP Publishing.
- [22] R. H. Hadfield, *Nature Photonics* **13**, 696 (2009).
- [23] V. Averchenko, D. Sych, G. Schunk, U. Vogl, C. Marquardt, and G. Leuchs, *Phys. Rev. A* **96**, 043822 (2017), publisher: American Physical Society.
- [24] D. F. V. James and P. G. Kwiat, *Phys. Rev. Lett.* **89**, 183601 (2002), publisher: American Physical Society.
- [25] A. Kuhn, M. Hennrich, and G. Rempe, *Phys. Rev. Lett.* **89**, 067901 (2002), publisher: American Physical Society.
- [26] C. W. Gardiner and M. J. Collett, *Physical Review A* **31**, 3761 (1985), publisher: American Physical Society.
- [27] N. F. Ramsey, *Phys. Rev.* **103**, 20 (1956), publisher: American Physical Society.
- [28] B. Q. Baragiola, R. L. Cook, A. M. Braczyk, and J. Combes, *Physical Review A* **86**, 013811 (2012), publisher: American Physical Society.

## SUPPLEMENTARY MATERIALS

### SOURCE

#### Quantum

In the interaction picture, the Hamiltonian describing the Raman model is

$$H = \hbar E(t) a^\dagger \sigma_+ + \hbar E^*(t) \sigma_- a, \quad (7)$$

where  $a$  is the internal cavity mode and  $\sigma_\pm$  are the raising and lowering operators in the subspace formed  $|g\rangle$  and  $|e\rangle$ . At a finite temperature, the evolution of the cavity-atomic joint state is governed by the master equation

$$\frac{d\rho}{dt} = -i[H, \rho] + \kappa(\bar{n} + 1) \mathcal{D}[a]\rho + \kappa\bar{n} \mathcal{D}[a^\dagger]\rho \quad (8)$$

where  $\kappa$  is the decay rate into the environment at mean photon number  $\bar{n} = (e^{\hbar\omega_a/k_bT} - 1)^{-1}$ . We have neglected the decay  $|e\rangle \rightarrow |g\rangle$  with the assumption the atomic decay rate is much slower than that of the interactivity mode. We use the quantum Langevin equations to describe the stochastic evolution of the intracavity  $a$  in terms of the input  $a_i$  [18, 26]

$$\frac{da}{dt} = -iE(t)\sigma_+ - \frac{\kappa}{2}a + \sqrt{\kappa}a_i. \quad (9)$$

Assuming the cavity and input modes are initially in a thermal states where  $\langle a(0) \rangle = 0$ . We can now solve Eq.(9) and obtain the amplitude of the cavity output mode

$$\langle a_o(t) \rangle = -i\sqrt{\kappa} \int_0^t e^{\frac{\kappa}{2}(t-t')} E(t') \langle \sigma_+(t') \rangle. \quad (10)$$

Thus the output is—on average—the convolution of the cavity response and the product of the control field amplitude and atomic polarisation. As we can control  $E(t)$  externally we can shape the overall response of the source.

Likewise the photon flux emitted into the output mode can be ascertained using the input-output relations

$$\langle a_o^\dagger(t) a_o(t) \rangle = \kappa \langle a^\dagger a \rangle - \sqrt{\kappa} \langle a^\dagger a_i + a_i^\dagger a \rangle + \langle a_i^\dagger a_i \rangle. \quad (11)$$

A reliable single photon source will operate in the limit of a large cavity decay rate. Single photons excited in the cavity are most likely to be emitted via the output mirror rather than coherently absorbed by the atomic system. In principle we are able to adiabatically eliminate the cavity dynamics in the long term limit and the cavity field becomes tethered to the atomic polarisation. This implies that we can replace cavity operator as  $a \rightarrow -2iE(t)\sigma_+/\kappa + 2a_i/\sqrt{\kappa}$ . In this limit the the output photon flux is given by

$$\langle a_o^\dagger(t) a_o(t) \rangle = \langle a_i^\dagger a_i \rangle + \frac{2i}{\sqrt{\kappa}} \langle E(t) a_i^\dagger \sigma_+ - E^*(t) \sigma_- a_i \rangle. \quad (12)$$

The master equation describing the atomic system alone can be written in this limit as

$$\mathcal{L}\rho^{(\sigma)} = \frac{4(\bar{n}+1)I(t)}{\kappa}\mathcal{D}[\sigma_+]\rho^{(\sigma)} + \frac{4\bar{n}I(t)}{\kappa}\mathcal{D}[\sigma_-]\rho^{(\sigma)}, \quad (13)$$

where  $\rho^{(\sigma)}$  describes the quantum state of the atom alone. From the atomic Langevin equations, we compute the general solution to  $\sigma_+(t)$

$$\sigma_+(t) = -\frac{2i}{\sqrt{\kappa}} \int_0^t dt' e^{\frac{\kappa}{2}(t-t')} \sigma_z(t') a_i(t') E^*(t') \quad (14)$$

Multiplying this expression by  $a_i^\dagger$  from the right and making use of the commutation relation  $[a_i(t), a_i^\dagger(t')] = \delta(t-t')$  and the integral identity  $\int_0^t \delta(t-t') f(t') dt' = f(t)/2$ , we can find the expression

$$\frac{2i}{\sqrt{\kappa}} \langle E(t) a_i^\dagger \sigma_+ - E^*(t) \sigma_- a_i \rangle = \frac{4I(t)}{\kappa} \langle \sigma_z(t) \rangle. \quad (15)$$

Using the fact that  $\sigma_z = 1 - 2\sigma_- \sigma_+$ , we can find the general average evolution by computing the probability of measuring a photon in the ground state where  $\langle \sigma_- \sigma_+ \rangle = P_g(t)$ . Using the atomic master equation we obtain

$$\frac{dP_g(t)}{dt} = -\frac{4I(t)}{\kappa} (2\bar{n}+1)P_g(t) + \frac{4I(t)\bar{n}}{\kappa} \quad (16)$$

which has the general solution—given the initial condition  $P_g(0) = (1 + e^{-\mu\sigma})^{-1}$

$$P_g(t) = \frac{e^{-\tau}(1 + \bar{n}) + \bar{n}}{2\bar{n} + 1} - \frac{e^{-\tau}}{1 + e^{\mu\sigma}} \quad (17)$$

where  $\tau = (4/(2\bar{n}+1)\kappa) \int_0^t dt' I(t')$  and approaches 0 in the long time limit at zero temperature corresponding to a perfect emission. The expectation value of  $\sigma_z(t)$  in the long time limit where  $t \gg 0$

$$\langle \sigma_z(t) \rangle = \frac{1}{1 + 2\bar{n}} = \tanh\left(\frac{\hbar\omega}{2k_B T}\right), \quad (18)$$

which describes the mean atomic polarisation of an atom in a thermal bath as expected. Recombining our expression for  $\langle \sigma_z \rangle$  and the mean photon number in the input mode the cavity  $\langle a_i^\dagger a_i \rangle$ , we obtain the expression for the mean photon number in the output mode Eq. (12) as

$$\langle a_o^\dagger(t) a_o(t) \rangle = \bar{n} + \frac{4I(t)}{\kappa} \langle \sigma_z(t) \rangle \quad (19)$$

which at zero temperature corresponds to the expected result for a single photon pulse.

### Classical

The classical model is effectively described by the agent emitting a coherent pulse with temporal profile  $E(t)$ . For

an environment initially in a thermal state with a mean photon number  $\bar{n}$ , the mean amplitude is given by

$$\langle a_o(t) \rangle = -i \int_0^t dt' E(t'), \quad (20)$$

and the mean photon number in the environment is given by

$$\langle a_o^\dagger(t) a_o(t) \rangle = \bar{n} + \int_0^t I(t') dt'. \quad (21)$$

## DETECTOR

### Quantum

We can now repeat our analysis in the previous but make our detector inefficient and assuming it is in thermal equilibrium with a thermal bath with mean photon number  $\bar{n}$ . We start by assuming that the initial state is

$$\rho_{\text{sys}}(0) = \frac{e^{-\mu_a a^\dagger a}}{Z_a} \otimes \frac{e^{\mu_\sigma \sigma_z/2}}{Z_\sigma} \quad (22)$$

The sign of the atomic ensemble has now change reflecting the fact that the detector is effectively maintained at a negative temperature. We consider the Fock state master equations [28] including an additional multiplicative factor of  $\sqrt{\eta}$  where  $\eta$  is the quantum efficiency of the detector. The whole system including the incoming Fock mode from the environment can be accounted for in the initial state  $\rho = \rho_{\text{sys}}(0) \otimes |1_\xi\rangle\langle 1_\xi|$  which obeys the ME

$$\begin{aligned} \dot{\rho}_{nm} = & \mathcal{L}\rho_{nm} + \sqrt{\bar{n}}\sqrt{\eta\kappa}\xi(t) [\rho_{n-1,m}, a^\dagger] \\ & + \sqrt{\bar{m}}\sqrt{\eta\kappa}\xi^*(t) [a, \rho_{n,m-1}]. \end{aligned} \quad (23)$$

The off-diagonal elements of the Fock state master equation are initialised to 0 whereas the diagonal elements are initialised to  $\rho(0)$ . Only the top density operator  $\rho_{11}$  is required to compute expectation values. The superoperator further includes thermal excitations yielding the master equation

$$\begin{aligned} \mathcal{L}\rho = & -i [V(t)a^\dagger\sigma_+ + V^*(t)\sigma_-a, \rho] + \kappa(\bar{n}+1)\mathcal{D}[a]\rho \\ & + \kappa\bar{n}\mathcal{D}[a^\dagger]\rho, \end{aligned} \quad (24)$$

where  $V(t)$  is the drive field of the sensor. We repeat the method as earlier by making the adiabatic approximation  $a = -2iV(t)\sigma_+/\kappa - 2\xi(t)/\sqrt{\kappa}$  and eliminating the cavity dynamics yielding the new ME

$$\mathcal{L}\rho^{(\sigma)} = \frac{4(\bar{n}+1)I_V(t)}{\kappa}\mathcal{D}[\sigma_+]\rho^{(\sigma)} + \frac{4\bar{n}I_V(t)}{\kappa}\mathcal{D}[\sigma_-]\rho^{(\sigma)}, \quad (25)$$

where  $I_V(t) = |V(t)|^2$ . The Fock state ME for the atomic system alone becomes

$$\begin{aligned} \dot{\rho}_{nm}^{(\sigma)} = & \frac{4I(t)}{\kappa}\mathcal{D}[\sigma_+]\rho_{nm}^{(\sigma)} + \frac{2i\sqrt{\eta}}{\sqrt{\kappa}} \left( \sqrt{\bar{n}}\xi(t)E^*(t) [\rho_{n-1,m}^{(\sigma)}, \sigma_-] \right. \\ & \left. - \sqrt{\bar{m}}\xi^*(t)E(t) [\sigma_+, \rho_{n,m-1}^{(\sigma)}] \right) \end{aligned} \quad (26)$$

We can now compute the probability of finding the atom in the ground state  $P_g(t) = \langle \sigma_- \sigma_+ \rangle$

$$\begin{aligned} \frac{dP_g(t)}{dt} = & -\frac{4I_V(t)}{\kappa}(2\bar{n}+1)P_g(t) + \frac{4I_V(t)\bar{n}}{\kappa} \\ & + \frac{2i\sqrt{\eta}V^*(t)\xi(t)}{\sqrt{\kappa}}\langle \sigma_- \rangle_{01} - \frac{2i\sqrt{\eta}V(t)\xi^*(t)}{\sqrt{\kappa}}\langle \sigma_+ \rangle_{10} \end{aligned} \quad (27)$$

We must now find  $\langle \sigma_- \rangle_{01}$  which can be found by solving

$$\frac{d\langle \sigma_- \rangle_{01}}{dt} = -\frac{2(2\bar{n}+1)I(t)}{\kappa}\langle \sigma_- \rangle_{01} - \frac{2i\xi^*(t)V(t)}{\sqrt{\kappa}}\langle \sigma_z \rangle_{00}, \quad (28)$$

We must lastly find the evolution of  $\langle \sigma_z \rangle_{00}$ . Given the sensor is being maintained in a negative temperature state, the probability of finding it in the ground state when the environment is in the vacuum is  $P_g(t)_{00} = 1/(1+e^{\mu\sigma})$ . We can now substitute this result into  $\langle \sigma_- \rangle_{01}$  and using the initial condition  $\langle \sigma_- \rangle_{01}(0) = 0$  and obtain the general solution

$$\langle \sigma_- \rangle_{01}(t) = -2i\sqrt{\frac{\eta}{\kappa}} \int_0^t e^{(\tau'-\tau)V(t')\xi^*(t')} \tanh\left(\frac{\mu\sigma}{2}\right) dt', \quad (29)$$

where  $\tau_f = 2 \int_0^t dt' (1+2n)I_V(t')/k$ . Substituting this result into our differential equation for  $P_g(t)$  we obtain

$$\frac{dP_g(t)}{dt} = -\frac{4I_V(t)}{\kappa}(2\bar{n}+1)P_g(t) + \frac{4I_V(t)\bar{n}}{\kappa} + \frac{4\eta}{\kappa(1+2\bar{n})} \left( V^*(t)\xi(t) \int_0^t e^{(\tau'-\tau)V(t')\xi^*(t')} dt' + H.C \right) \quad (30)$$

which yields the general solution

$$P_g(t) = \frac{1}{2\bar{n}+1} \left( \bar{n} + \frac{4\eta}{\kappa} \left| \int_0^t dt' e^{(\tau'-\tau)V(t')\xi^*(t')} \right|^2 \right). \quad (31)$$

When  $\kappa$  is large and the response function becomes close to instantaneous we can rearrange the expression to obtain

$$P_g(t) = \frac{1}{1+e^{\mu\sigma}} + \frac{4\eta\Gamma}{\kappa} \tanh\left(\frac{\mu\sigma}{2}\right). \quad (32)$$

where  $\Gamma = \left| \int dt' V^*(\vec{k}, t')\xi(k, t') \right|^2$ . Moreover, it is quite clear that the first term in this expression corresponds to the conditional probability of the atom transitioning to the ground state via an absorption of a thermal photon, whereas the second term from the incoming Fock mode. Thus, we can express this probability as a sum of the two conditional cases

$$P_g(t) = P_{g|T}(t) + P_{g|\xi}(t) \quad (33)$$

where  $T$  signifies a thermal photon and  $\xi$  our signal photon.

### Semi-classical - Coherent pulse

We can consider a semi-classical model of the detector whereby the incoming mode is no longer in a Fock state but a coherent state  $\rho = \rho_{\text{sys}}(0) \otimes |\alpha_\xi\rangle\langle\alpha_\xi|$  with  $|\alpha_\xi|^2 = 1$ .

Given that the coherent state is a eigenstate of the annihilation operator, the Fock-state master equations reduce to the standard master equation with an additional time dependent coherent drive

$$\begin{aligned} \mathcal{L}\rho = & -i[V(t)a^\dagger\sigma_+ + V^*(t)\sigma_-a, \rho] + \kappa(\bar{n}+1)\mathcal{D}[a]\rho \\ & + \kappa\bar{n}\mathcal{D}[a^\dagger]\rho - i\sqrt{\eta\kappa}[i\xi^*(t)a - i\xi(t)a^\dagger, \rho]. \end{aligned} \quad (34)$$

We can now repeat our analysis by again adiabatically eliminating the cavity which yields the familiar atomic master equation Eq. (25) with a coherent driving term

$$\begin{aligned} \mathcal{L}\rho^{(\sigma)} = & \frac{4(\bar{n}+1)I(t)}{\kappa}\mathcal{D}[\sigma_+]\rho^{(\sigma)} + \frac{4\bar{n}I(t)}{\kappa}\mathcal{D}[\sigma_-]\rho^{(\sigma)} \\ & - \frac{2i\sqrt{\eta}}{\sqrt{\kappa}} \left[ V(t)\xi^*(t)\sigma_+(t) + V^*(t)\xi(t)\sigma_-(t), \rho^{(\sigma)} \right]. \end{aligned} \quad (35)$$

Using this result, we can now compute the expectation value  $P_g(t)$

$$\begin{aligned} \frac{dP_g(t)}{dt} = & -\frac{4I_V(t)}{\kappa}(2\bar{n}+1)P_g(t) + \frac{4I_V(t)\bar{n}}{\kappa} \\ & + \frac{2i\sqrt{\eta}V^*(t)\xi(t)}{\sqrt{\kappa}}\langle \sigma_- \rangle - \frac{2i\sqrt{\eta}V(t)\xi^*(t)}{\sqrt{\kappa}}\langle \sigma_+ \rangle. \end{aligned} \quad (36)$$

We again find the equation of motion for the lowering operator  $\langle \sigma_- \rangle$  using the above ME

$$\frac{d\langle \sigma_- \rangle}{dt} = -\frac{2(2\bar{n} + 1)I_V(t)}{\kappa} \langle \sigma_- \rangle - \frac{2i\sqrt{\eta}\xi^*(t)V(t)}{\sqrt{\kappa}} (1 - 2P_g(t)). \quad (37)$$

A general solution to this DE can be determined using the initial condition  $\langle \sigma_-(0) \rangle = 0$

$$\langle \sigma_- \rangle = -2i\sqrt{\frac{\eta}{\kappa}} \int_0^t e^{(\tau' - \tau)} V(t') \xi^*(t') (1 - 2P_g(t')) dt'. \quad (38)$$

---


$$\frac{dP_g(t)}{dt} = -\frac{4I_V(t)}{\kappa} (2\bar{n} + 1)P_g(t) + \frac{4\bar{n}I_V(t)}{\kappa} + \frac{4\eta}{\kappa} \left( V(t)\xi^*(t) \int_0^t e^{(\tau' - \tau)} V(t') \xi^*(t') (1 - 2P_g(t)) dt' + H.C \right) \quad (39)$$

$$\Rightarrow P_g(t) = \frac{1}{1 + 2\bar{n}} \left( \bar{n} + \frac{4\eta}{\kappa} \left| \int_0^t dt' e^{(\tau' - \tau)} V(t') \xi^*(t') \right|^2 e^{-4\eta \left| \int_0^t dt' e^{(\tau' - \tau)} V(t') \xi^*(t') \right|^2 / \kappa} \right) \quad (40)$$

If we again make the assumptions that  $\kappa$  is large and the response is approximately instantaneous, then the probability of finding the atom in the ground state is given as

$$P_g(t) = \frac{1}{1 + e^{\mu_\sigma}} + \frac{4\eta\Gamma}{\kappa} \tanh\left(\frac{\mu_\sigma}{2}\right) e^{-4\eta\Gamma/\kappa}, \quad (41)$$

Thus the general differential equation describing the evolution of  $\langle \sigma_z(t) \rangle$  after making a change of variables is

---


$$\text{where } \Gamma = \left| \int dt' V^*(\vec{k}, t') \xi(k, t') \right|^2.$$